Math. Model. Nat. Phenom.
Vol. 3, No. 1, 2008, pp. 108-125

Instabilities of diffuse interfaces

N. Bessonov[a], J. Pojman[b], G. Viner[b], V. Volpert[c1], B. Zoltowski[b]

[a] Institute of Mechanical Engineering Problems, 199178 Saint Petersburg, Russia
[b] Department of Chemistry and Biochemistry, The University of Southern Mississippi
Hattiesburg, MS 39606, USA
[c] Institut de Mathématiques, UMR 5208 CNRS, Université Lyon 1
69622 Villeurbanne, France

Abstract. Composition gradients in miscible liquids can create volume forces resulting in various interfacial phenomena. Experimental observations of these phenomena are related to some difficulties because they are transient, sufficiently weak and can be hidden by gravity driven flows. As a consequence, the question about their existence and about adequate mathematical models is not yet completely elucidated. In this work we present some experimental evidences of interfacial phenomena in miscible liquids and numerical simulations of miscible drops and diffuse interfaces.

Key words: miscible liquids, interfacial phenomena, drops, interfacial waves
AMS subject classification: 76E17, 76R50

1. Effective interfacial tension in miscible liquids

The interfacial tension between immiscible fluids is an equilibrium thermodynamic property that results from the differences in intermolecular interactions between the two different types of molecules. However, when two miscible fluids are brought in contact, a large concentration (and density) gradient can exist, which relaxes through diffusion as the system approaches the uniform, equilibrium state. Because the molecules are different, there are necessarily differences in intermolecular interactions, which may lead to transient interfacial phenomena. In the 19th century there were reports of phenomena in which an effective interfacial tension (EIT) was invoked. (These are discussed by Joseph and Renardy [24]. Zeldovich published an excellent work in which

[1]Corresponding author. E-mail: volpert@math.univ-lyon1.fr

Article available at http://www.mmnp-journal.org or http://dx.doi.org/10.1051/mmnp:2008036

he derived from thermodynamics that an interfacial tension should exist between miscible fluids brought into contact [48]. Davis proposed that when two miscible fluids are placed in contact they will immediately begin to mix diffusively across the concentration front, and the composition inhomogeneities can give rise to pressure anisotropies and to a tension between the fluids [17]. Rousar and Nauman, following the work of Rowlinson and Widom [40] proposed that an interfacial tension can be found without assuming that the system is at equilibrium [38]. There have been several reports of phenomena in which the authors invoke an interfacial tension with miscible systems [18], [9], [29], [33], [42].

Isobutyric acid (IBA) and water exhibit an Upper Critical Solution Temperature (UCST) at 26.3 ^{0}C, which means that above the UCST the materials are miscible in all proportions but below it they form two phases [12], [13], [19], [39], [40]. By rapidly raising the temperature above the UCST, thermal equilibrium is achieved quickly but chemical equilibrium takes hours. Thus, two miscible fluids are created with a sharp well-defined transition zone between them. May and Maher were the first to report the measurement of an interfacial tension between miscible fluids using light scattering [28]. They started with the two phases 0.2 K below the UCST and then rapidly raised the system's temperature above its UCST. The interfacial tension was initially 0.0017 mN/m and then relaxed over two hours to 0.0002 mN/m. Vlad and Maher studied the cyclohexane-methanol system by the same technique and claimed that gravity slowed the expected rate of diffusion [45]. Cicuta et al. also contended that fluctuations measured by May and Maher and Vlad and Maher were not related to an interfacial tension but rather were instead nonequilibrium fluctuations associated with a diffuse gradient [14]. Cicuta et al. reported interfacial tensions for the aniline-cyclohexane system above its UCST using light scattering [14].

Spinning drop tensiometry has also been used to study fluids with critical behavior. Heinrich and Wolf studied the interfacial tension of coexisting phases of methylcyclohexane-polystyrene and cyclohexane-polystyrene within 0.5 K of the UCST and performed temperature-jump experiments [20], [21]. They also studied methylcyclohexane-polystyrene in a spinning drop tensiometer with temperature jumps but below the UCST [20], [21]. Petitjeans was the first to study miscible fluids with spinning drop tensiometry. SDT with miscible systems can be difficult to interpret because of the difficulty in separating interfacial effects from viscous relaxation of the drop. For example, Petitjeans reported an interfacial tension for a water drop in glycerin but it did not relax with time [31].

We propose that miscible systems can be divided into three types:

1) Miscible in all proportions, like honey and water, or dodecyl acrylate (DDA) and polydodecyl acrylate (pDDA), or ethanol and water. In such systems the width of the transition zone grows with time.

2) Partially miscible but not near a consulate point (LCST or UCST), like butanol and water [34]. The transition zone does not become wider nor does the EIT relax with time. The gradient is fixed by the solubility limit. Butanol can only penetrate into water up to the concentration equal to its solubility.

3) Systems near a consulate point, such as IBA-water above its Upper Critical Solution Temperature (UCST). The concentration gradient is sharp. The diffusion coefficient at the consulate point, i.e., the concentrations and temperature at the maximum of the IBA-water phase diagram, is

zero [10]. If the concentrations are on the either side of the UCST, the gradient is very sharp as it passes through the UCST.

In this work we will present the experimental results on SDT for the DDA - pDDA system and IBA - water (Section 2). The butanol - water systems differs from IBA - water by their thermodynamic properties but behavior of the two systems in the SDT appears to be qualitatively the same.

Theoretical investigations of miscible liquids begin with the work by Korteweg [25]. There are various approaches to the derivation of the mathematical model describing capillary forces in miscible liquids (see [1], [2] and references therein). They start from the assumption that the free energy density depends on the square of the density gradient or of the composition gradient. Some additional assumptions related to the thermodynamics of irreversible processes allow one to obtain the full set of equations from the conservation laws. Usually they contain the Cahn-Hilliard equation for the composition (order parameter) in the case of a binary mixture, the equations of motion with the Korteweg-like stresses, and the equation for the entropy production. Some simulations of miscible liquids are recently carried out in [5], [6], [11], [23], [24], [38], [46].

In the theoretical part of this work we will use the model based on the Korteweg stresses to study behavior of diffuse interfaces. In Section 3 we model the experiments presented in Section 2. We carry out numerical simulations of cylindrical jets in order to reveal the capillary instability in miscible liquids. We next study the evolution of the shape of rotating drops. In both cases, numerical results are in a good agreement with the experiments. In Section 4 we continue to study perturbations of diffuse interfaces. We show that they can form not only standing waves as in the case of capillary instability but also travelling waves propagating along the interface.

2. Spinning drop tensiometry

2.1. Vonnegut method

In 1942, Vonnegut developed the spinning drop method for measuring interfacial tension [47]. A capillary is filled with the more dense phase, and a drop of the less dense phase is injected. The capillary is rotated at a high rotation rate ($>$ 6,000 rpm). The drop reaches an equilibrium shape reflecting the balance between the interfacial energy and the rotational energy. If the drop length is at least four times longer than the drop radius, the interfacial tension can be determined from the drop radius as long as the difference in densities between the two fluids are known [41]:

$$\sigma = \frac{1}{4}\,\Delta\rho\omega^2 r^3.$$

Here $\Delta\rho$ is the density difference, ω is the angular velocity, r the radius of the cylindrical drop. To avoid complications from buoyancy, the drop rotation rate must be greater than a critical value [27], [15], [22].

Isobutyric acid (Aldrich, 99 %) and 1-butanol (Fisher Chemicals, 99.9 %) were used without further purification. All solutions were prepared using deionized water. In the case of the IBA - water system, IBA and water were allowed to equilibrate at room temperature. The capillary

was filled with the resulting aqueous phase and while it was rotating the temperature was lowered, and a drop of the IBA-rich phase was formed. The SDT was thermostated with a VWR 1166 circulator that flowed oil around the capillary. A temperature probe in the instrument provided the temperature to within 0.1 ^{0}C. The oil also served to lubricate the bearings. For the 1-butanol - water system, a drop ($\approx 10\mu L$) of pre-thermostated 1-butanol was injected in the thermostated capillary filled with deionized water. The measurements have been conducted in a temperature range between 9 ^{0}C and 60 ^{0}C. The density of 1-butanol in this range was taken from the literature.

2.2. Interfacial tension measurements

All the interfacial tension measurements have been conducted with a Krüss SITE100 Spinning Drop Tensiometer equipped with a digital camera. Krüss software DSAII was used for calibration and to operate the instrument (e.g., setting rotation speed). Experiments were recorded using a digital monochrome camera connected to the PC using DIVX compression. When a drop was long enough to meet the Vonnegut condition, the radius was measured but when the drop was too short both radius and length were measured, and the extended Vonnegut method was used.

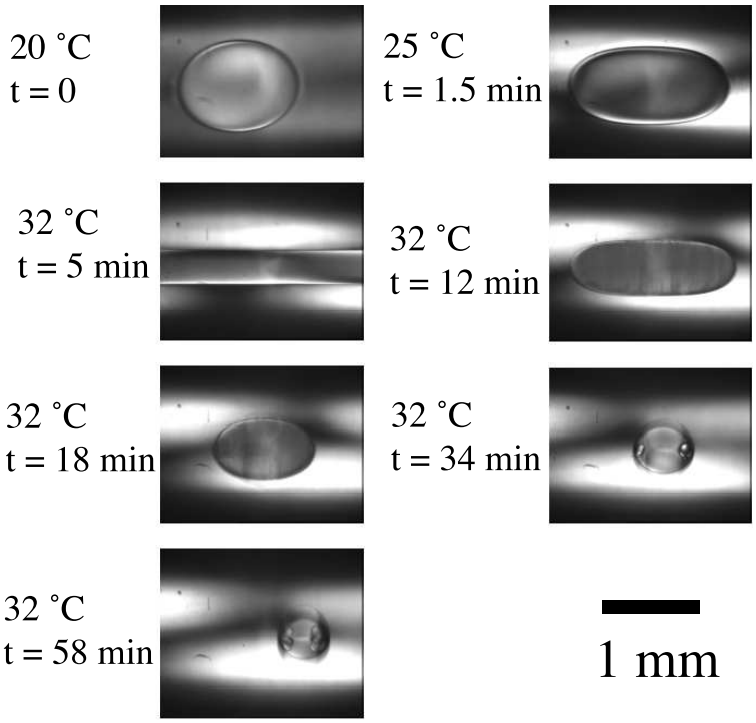

Figure 1: Time evolution of a drop of IBA-rich phase in a water-rich phase, before and after the jump in temperature, $\omega = 8000$ rpm.

IBA and water are partially miscible below 26.3 ^{0}C but miscible in all proportions above this Upper Critical Solution Temperature [12], [19]. A saturated solution of IBA in water was injected in the SDT capillary, and the temperature was lowered to 20 ^{0}C while the tensiometer was rotating.

After the IBA droplets separated from the solution and coalesced into one large drop, the temperature was raised. (We determined that thermal equilibrium was reached within 100 seconds from the time the bath reached the final temperature by observing the relaxation of 1-butanol-water drops. We performed temperature jumps for equilibrated 1-butanol in water and observed the amount of time required for the system to reach its new equilibrium.) We chose to use initial temperatures so far from the UCST to increase the concentration difference between the drop and the matrix. Also, decreasing the temperature from room temperature allowed a drop to form spontaneously and so no drop had to be injected.

Figure 1 shows a drop at different times. As the temperature is increased at 1.5 min, the drop lengthens because the interfacial tension decreases. After 5 minutes when the temperature reached 32 ^{0}C, the drop stretched significantly. The next images show the evolution of the drop shape in time. The transition zone between the phases remains sharp even as the drop dissolves into the matrix. It decreases and becomes spherical due to the effective interfacial tension. In the next section, we will see the same behavior in numerical simulations.

To demonstrate that an effective interfacial tension exists, we measured the radius as a function of rotation rate. From a plot of r^{-3} vs. ω^2 (Fig. 2), Pojman et al. determined the effective interfacial tension [34]. We confirmed this relationship for a single drop that was initially equilibrated at 24 ^{0}C. The temperature was raised to 28 ^{0}C. The EIT, assuming the density difference had not changed significantly because of diffusion, was 0.10×10^{-3} N/m. The interfacial tension for the equilibrium system at 24 ^{0}C was 0.14×10^{-3} N/m. For comparison, the interfacial tension for water is about 70×10^{-3} N/m.

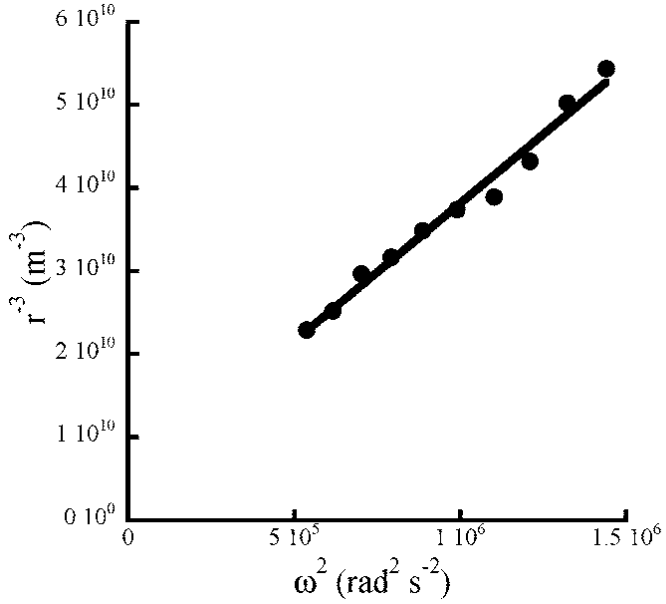

Figure 2: Graph r^{-3} vs. ω^2 at a final temperature of 28 ^{0}C for IBA-water originally equilibrated at 24 ^{0}C

2.3. Droplet breakup

Quirion and Pageau [37] demonstrated for immiscible systems that upon a large decrease in rotation rate, a capillary instability could be observed [43], [44]. Quirion and Pageau were able to measure the interfacial tension from the rate of the drop breakup. Figure 3 shows how the miscible drop breaks apart upon the rapid decrease in rotation rate from 7160 rpm to 1300 rpm for a drop of IBA-rich phase in water-rich phase at 30 ^{0}C; the phases were formed at 15 ^{0}C. This result provides evidence that an effective interfacial tension does exist between the unequilibrated phases of IBA and water.

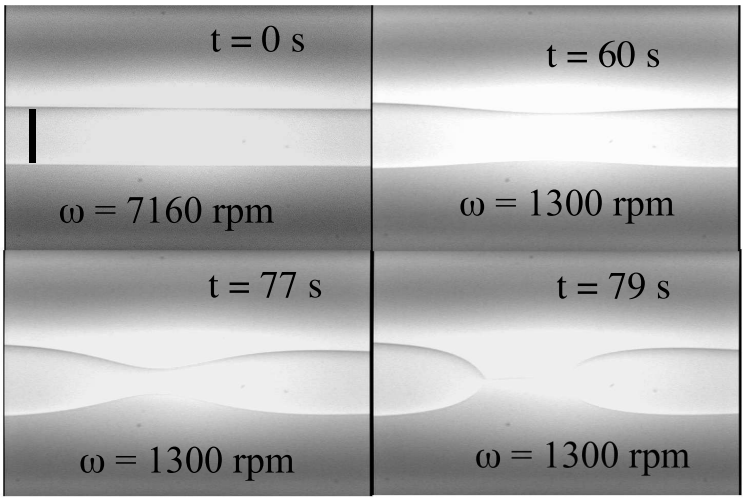

Figure 3: Image of droplet breakup after the rotation rate was decreased from 7160 to 1300 rpm. Scale bar corresponds to 4.7×10^{-4} m. The initial temperature was 15 ^{0}C. The temperature was jumped to 30 ^{0}C. Five minutes after the temperature jump, the rotation rate was rapidly decreased.

2.4. Dodecyl acrylate in poly(dodecyl acrylate)

Several systems that are miscible in all proportions have been studied. Petitjeans studied glycerol in water by a fluid displacement experiment [33] and using spinning drop tensiometry [31], [32]. Pojman et al. supervised an experiment on the International Space Station to study the behavior of honey and water and were able to put an upper bound on the value of the Korteweg stress parameter for that system [35]. Zoltowski et al. studied a monomer that is miscible in its polymer [49]. This system relates to simulations performed on a polymer system showing how convection could be caused by gradients in the effective tension between a monomer and its miscible polymer [7].

The temporal evolution of the drop shape can be complicated. The drops never were simple cylinders with hemispherical ends as seen with immiscible fluids. The drops continuously stretched

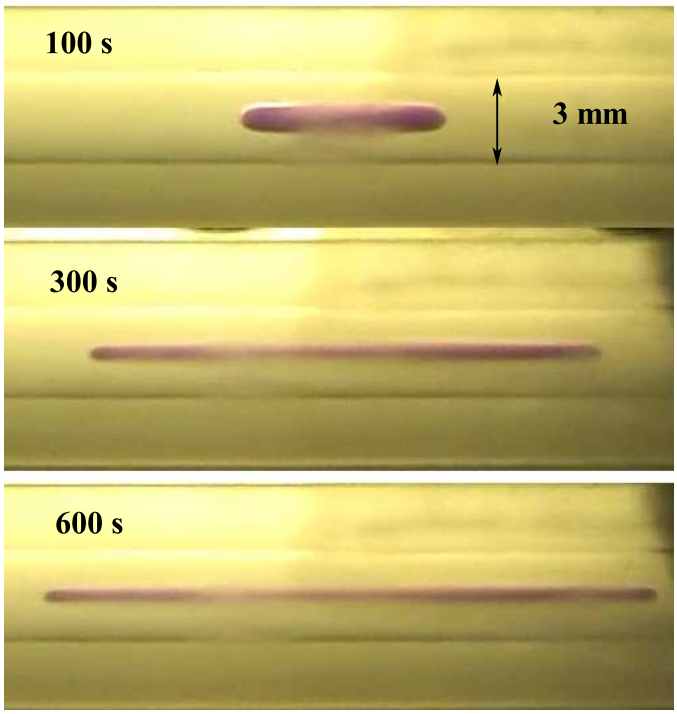

Figure 4: A drop of dodecyl acrylate (containing the dye meso zinc- tetraphenylporphine) in a matrix of low molecular weight (14,000) but viscous poly(dodecyl acrylate). The rotation rate in the SDT is 6,000 rpm and the temperature is 25 ^{0}C

with time as seen in Figure 4. There was also an issue of what diameter of the drop should be used since a drop-with-in a drop was imaged (Figure 5). Measurements using the inner diameter and outer diameter provided confirmation of the existence of an effective interfacial tension (EIT). By observing between 500 and 1500 s, they confirmed that the measured EIT was independent of rotation rate beyond 6,000 rpm. Such a rotational dependence is also seen with immiscible systems. They observed that interfacial width did not grow with the expected $\sqrt{t}$ dependence although the DDA-pDDA system was previously shown to follow Fick's law in a static configuration [3]. We proposed that diffusion weakens the EIT, which allows the drop to stretch. As the drop stretches, the interfacial width contracts and so the EIT remains relatively constant. The EIT was found to decrease with temperature and increase with the difference in concentration between the monomer drop and polymer-monomer bulk fluid. The square gradient parameter, k, was determined from EIT $= k(\Delta c)^2/\delta$ where Δc was the difference in mole fraction, and δ was the width of the transition zone. The square gradient parameter was on the order of 10^{-9} N. The square gradient parameter was found to decrease with temperature, it was independent of concentration but increased with the molecular weight of the polymer.

It was necessary to verify that the behavior of the DDA-pDDA system was due to the EIT and not to the high viscosity of the polymer. This was done by estimating the mechanical relaxation time for an immiscible analog of DDA involving the viscous polymer as the bulk solution.

Small chain primary alcohols are particularly well suited as immiscible analogs, because they have comparable interfacial tensions and differences in densities. The relaxation time was estimated by subjecting the 1-propanol drop to a series of rotation jumps and was taken as the amount of time necessary for the drop to reach the mechanical equilibrium, which was about 50 seconds. Therefore, the mechanical relaxation time is much less than the time of the experiment (cf. Figure 4).

An important difference between the DDA-pDDA system and IBA-water and butanol-water was the behavior of the drop with changes in rotation. The monomer drop did not contract when the rotation rate was decreased as would be expected if there were an interfacial tension and as was seen in the IBA-water system. Both the IBA-water and 1-butanol-water system exhibited a linear dependence between r^{-3} and ω^2, irrespective if the rotation rate was increased or decreased. However, the viscosity for the bulk phase in the other studies (essentially, water) was two orders of magnitude lower than the viscosity of the polymer. There are two possible explanations, viz., no EIT exists in the DDA-pDDA system or the EIT is too weak to overcome the viscous drag.

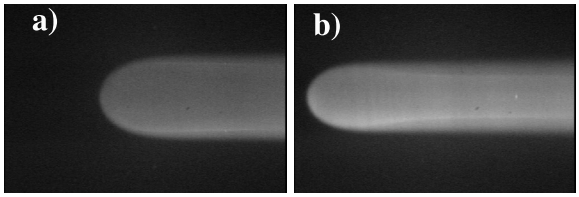

Figure 5: a) Image of drop after 200 seconds. b) Image of drop after 400 seconds. Field of view is 1.7 mm in the vertical direction

3. Simulations of miscible drops

In this section we model the experimental results presented above. We begin with the break up of a miscible drop in the IBA-water system. We will use here the model based on the Korteweg stresses which is derived to describe the motion of binary fluids [1], [2]. After that we use a simplified model in order to describe the evolution of the drop shape after the temperature increase (see Section 2.2).

3.1. Capillary instability

Consider a mixture of two miscible fluids and denote by c their composition, that is the function that changes between 0 and 1 and such that $c = 0$ corresponds to one pure fluid and $c = 1$ to another one. If the fluids are incompressible and have the same densities, then the evolution of the composition can be described by the diffusion equation with convective terms and Navier-Stokes equations with the Korteweg stresses:

$$\frac{\partial c}{\partial t} + v.\nabla c = d\Delta c, \tag{3.1}$$

$$\frac{\partial v}{\partial t} + (v.\nabla)v = -\frac{1}{\rho}\nabla p + \nu\Delta v - \frac{K}{\rho}\,\nabla c\,\Delta c, \quad \text{div } v = 0. \tag{3.2}$$

Here v is the fluid velocity, p the pressure, ρ the density, K the Korteweg parameter which characterizes the intensity of the volume force resulting from the inhomogeneous composition distribution.

Consider system (3.1), (3.2) in the 3D case. The initial distribution of the two liquids represents two long co-axial cylinders, one with a small diameter (2 mm) and another one with a larger diameter (10 mm). They are separated by a sharp interface. The boundary conditions at the outer surface are no-slip conditions for the velocity and no-flux condition for the composition. Numerical resolution of this problem is based on the velocity - pressure formulation with finite volume elements and adaptive mesh. The details of the numerical methods are presented in [5].

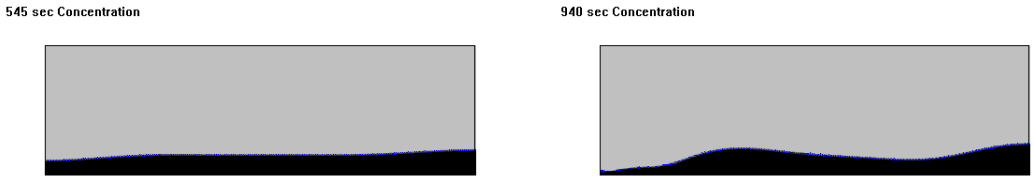

(a) (b)

Figure 6: Capillary instability in the case of a weak diffusion (numerical simulations).

The results of the numerical simulations are shown in Figure 6 (vertical section of the horizontal cylinder). The inner liquid is black, the outer liquid is grey. For the initial distribution, the interface separating them is horizontal. The left figure shows the beginning of the evolution where the interface becomes slightly curved. The instability becomes more pronounced with time (right figure). This effect is observed if the diffusion coefficient is sufficiently small (10^{-7} kg/(m· s)).

Thus, miscible liquids can manifest the capillary instability. The results of the numerical simulations are related to the experimental observations described in Section 2 though their correspondence is not exact. First of all, these are not simulations of the SDT, that is we do not take into account drop rotation in the model. The capillary instability is observed experimentally for the IBA - water system where the width of the interface remains constant. In the numerical simulations the width slowly grows because of the diffusion.

3.2. Simulations of rotating drops

In this section we model rotating drops using a quasi-stationary approximation. We assume that the drop of the inner liquid is in the mechanical equilibrium, that is the centrifugal force is counterbalanced by the interfacial tension at each moment of time. The interface between the two liquids has a constant width, and the inner liquid can diffuse through the interface. Therefore, the drop decreases with time, and its shape changes in such a way that it remains in the mechanical equilibrium. We suppose that the two liquids have different densities ρ_1 and ρ_2 (let $\rho_2 > \rho_1$) and rotate

around the x-axis with the angular velocity ω (Figure 7, left). It is clear that the first liquid will be located inside the second liquid. There is an interfacial tension σ at the interface between them.

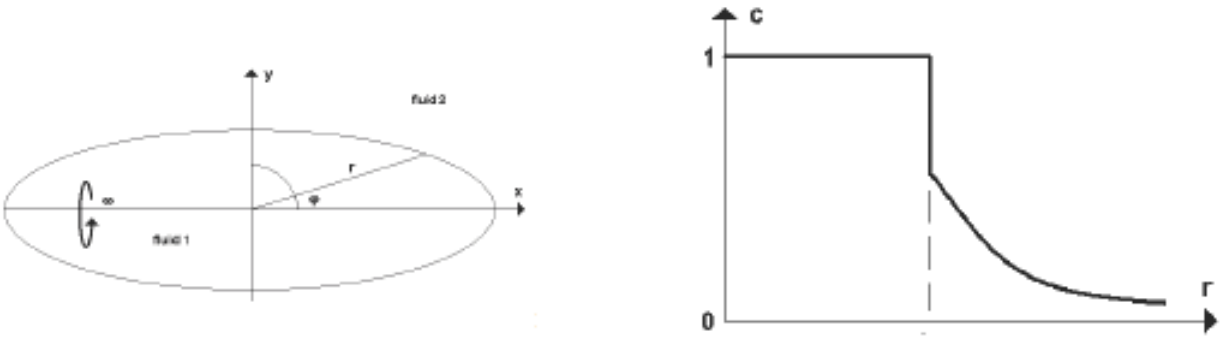

Figure 7: Description of the model.

Let us introduce the concentration c and suppose that $c = 1$ corresponds to liquid 1, $c = 0$ to liquid 2, and $0 < c < 1$ to the transition zone. In the case where the motion of the liquids is sufficiently slow and the transition zone is sufficiently narrow, the equation of the equilibrium of the interface can be written in the form:

$$\frac{yr}{l^2}\frac{d^2r}{d\phi^2} + \left(\cos\phi - \frac{2y}{l^2}\frac{dr}{d\phi}\right)\frac{dr}{d\phi} - \left[\left(\frac{2y^2l}{B} - \frac{r^2}{l^2} - 1\right)\sin\phi\right] r = 0, \tag{3.3}$$

where $y = r\sin\phi$, $l = \sqrt{(dr/d\phi)^2 + r^2}$, $B = 4\sigma/(R^3\omega^2\Delta\rho)$, R is the initial radius of the drop of fluid 1, that is the volume of fluid 1 equal $4\pi R^3/3$, $\Delta\rho = \rho_2 - \rho_1$.

Equation (3.3)) is written in the non-dimensional form, that is the value r in the (3.3) is non-dimensional and scaled by R. In the case where the liquids are immiscible, the solution $r(\phi)$ of equation (3.3) describes an exact form of the interface for a given value of the parameter B.

Figure 8: Simulations of a miscible drop with a sharp interface.

In the case where the liquids diffuse one into another, the effective interfacial tension σ can be found by the integration of the Korteweg force through the interface. The parameter B in this

case depends on ϕ since the concentration profile can be different at different parts of the interface. At the same time, we should take into account the change of R (entering B) resulting from the diffusion of the internal liquid and the decrease of the drop volume. We can assume that the interface is located where $c = 0.5$. Finally, in the case where only the first liquid can diffuse into the second one, the concentration distribution has the form shown in Figure 7, right. There is a jump of the concentration from $c = 1$ at the left to some given value $c = c_0$ at the right. To the right of the jump the concentration distribution is described by the diffusion equation. The interfacial tension in this case has two components: the classical interfacial tension related to the concentration jump and effective interfacial tension described by the Korteweg forces in the region where the concentration distribution is continuous.

We carry out numerical simulations for the case where only the inner liquid can diffuse through the interface, and the interfacial tension is determined by the concentration gradient at the interface. The shape of the drop of the inner liquid in consecutive moments of time is shown in Figure 8. Its volume decreases in time and its shape becomes closer to a circle. A similar behavior is observed experimentally for the IBA - water (Figure 1) and butanol - water (not shown here). We note that the centrifugal force is proportional to the drop volume while the capillary force to its surface. Hence the shape of small drops will be closer to the circle than the shape of large drops. This conclusion is in agreement with the experimental and numerical results.

4. Interfacial waves

Interfacial waves represent another type of instability of diffuse interfaces compared with the capillary instability discussed in the previous section. Consider a plane interface between two liquids and suppose that its width differs in space. Then the effective interfacial tension, which is in the inverse proportion to the interface width, also varies in space creating a force directed along the interface. This force can lead to the motion of the interface and of the neighboring liquid. Experimentally this effect can be observed if we change locally the interfacial tension by adding some chemicals or by heating the interface.

4.1. Stability analysis

We begin with a model problem where system (3.1), (3.2) is considered in the strip $\{-\infty < x < \infty,\ 0 \le y \le 1\}$ with the boundary conditions

$$y = 0:\ c = 0,\ \frac{\partial v_x}{\partial y} = 0, v_y = 0;\quad y = 1:\ c = 1,\ \frac{\partial v_x}{\partial y} = 0, v_y = 0. \tag{4.1}$$

In this case, this problem has a stationary solution $c = y, v_x = v_y = 0$. We linearize it about this solution:

$$\frac{\partial c}{\partial t} + v_y = d\Delta c, \tag{4.2}$$

$$\frac{\partial v_x}{\partial t} = -\frac{1}{\rho}\frac{\partial p}{\partial x} + \nu\Delta v_x, \tag{4.3}$$

$$\frac{\partial v_y}{\partial t} = -\frac{1}{\rho}\frac{\partial p}{\partial y} + \nu\Delta v_y - K\ \Delta c, \tag{4.4}$$

$$\frac{\partial v_x}{\partial x} + \frac{\partial v_y}{\partial y} = 0. \tag{4.5}$$

$$y = 0:\ c = 0,\ \frac{\partial v_x}{\partial y} = 0, v_y = 0;\ \ y = 1:\ c = 0,\ \frac{\partial v_x}{\partial y} = 0, v_y = 0. \tag{4.6}$$

et look for solution of problem (4.2)-(4.6) in the following form:

$$c = a\sin(ky)e^{imx}e^{\lambda t},\ v_x = b\cos(ky)e^{imx}e^{\lambda t},\ v_y = f\sin(ky)e^{imx}e^{\lambda t},\ p = g\cos(ky)e^{imx}e^{\lambda t},$$

where the wavenumber k is chosen to satisfy the boundary conditions. The condition of nontrivial solvability allows us to find the eigenvalue λ:

$$\lambda = -s^2(d+\nu) \pm \sqrt{\left(s^2(d-\nu)\right)^2 - Km^2}\ ,$$

where $s^2 = (k^2+m^2)/2$. If the diffusion coefficient and the viscosity are positive, then the solution exponentially decays. However, if they are small enough, the decay is slow and during some time the solution is close to the solution for $d = \nu = 0$. In this case, $\lambda = \pm i\sqrt{Km^2}$, and the solution behaves like $\cos(m(x \pm \sqrt{K}t))$. Thus for d and ν sufficiently small, there are waves propagating to the left and to the right with the velocity determined by the Korteweg constant K.

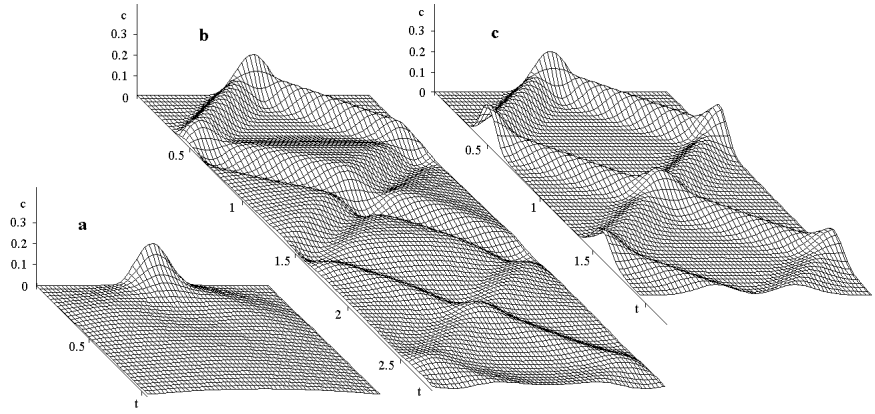

Figure 9: Evolution of the solution: a) $d = 10^{-2}$ cm^2/s, $\nu = 10^{-2}$ cm^2/s; b) $d = 10^{-5}, \nu = 10^{-3}$; c) $d = 10^{-2}, \nu = 10^{-3}$

4.2. Reduction to 1D problem

We begin with a model problem that allows us to study behavior of solutions inside the transition zone [4]. We look for the solution of (3.1), (3.2) in the form

$$v_x = u(x,t),\ v_y = yw(x,t),\ c = \frac{y}{\sqrt{K}}z(x,t),\ p = \rho\left(\frac{1}{2}y^2G(x,t) + \pi(x,t)\right).$$

and equate the terms with the same powers of y. We reduce (3.1), (3.2) to the system

$$\frac{\partial z}{\partial t} + u\frac{\partial z}{\partial x} - z\frac{\partial u}{\partial x} = d\frac{\partial^2 z}{\partial x^2}, \tag{4.7}$$

$$\frac{\partial u}{\partial t} + u\frac{\partial u}{\partial x} - z\frac{\partial z}{\partial x} = F + \nu\frac{\partial^2 u}{\partial x^2}, \tag{4.8}$$

$$\frac{\partial F}{\partial x} = G_0 + 2\left((\frac{\partial u}{\partial x})^2 - (\frac{\partial z}{\partial x})^2\right). \tag{4.9}$$

We consider problem (3.1), (3.2) in the strip $0 \le x \le 1$, $-\infty < y < \infty$ with the boundary conditions $x = 0, 1 : v_x = v_y = 0$, $\frac{\partial c}{\partial x} = 0$. The boundary conditions in the new variables become

$$x = 0, 1 : u = 0, \quad \frac{\partial u}{\partial x} = 0, \quad \frac{\partial z}{\partial x} = 0. \tag{4.10}$$

We note that (4.7)-(4.10) is the system with respect to the unknown functions z, u, F. It contains two second order equations, one first order equation, and 6 boundary conditions. The function $G_0(t)$ should be chosen to satisfy the boundary conditions.

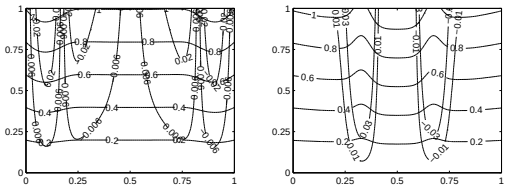

(a) (b)

Figure 10: Level lines of the composition and of the stream function after: (a) 0.4 s, (b) 0.8 s; $d = 10^{-5}$ cm^2/s, $\nu = 10^{-3}$ cm^2/s

Numerical simulations show existence of waves. When the wave comes to the boundary, it reflects from it and goes in the opposite direction. Figures 9 a - 9 c show the time evolution of the z component of the solution. If d and ν are sufficiently large, then the perturbation rapidly decays and the solution converges to a spatially homogeneous distribution (Fig. 9 a).

For the same d and for ν sufficiently small, there appears two waves propagating in the opposite directions, reflecting from the walls, going towards each other and so on periodically in time with a slowly decreasing amplitude (Fig. 9 c). If d is much smaller than ν, then the structure of waves is different compared with the previous case. The beginning of their evolution is the same, but after reflecting from the walls the sign of the perturbation changes: it is not the maximum of z which propagates but its minimum (Fig. 9 b).

Fig. 10 shows level lines of the composition c and of the stream function $\psi = yu$ at two fixed moments of time, before and after the first reflection from the walls. The particular form of the solution, which is linear in y, implies that the level lines of the stream function are not closed. There are two vortices propagating in the opposite directions. They come to the walls reflect from them and at the same time change the sign, i.e., the direction of fluid motion. They come towards each other, disappear when they meet, and appear again propagating in the opposite directions. This scenario repeats periodically with decreasing amplitude.

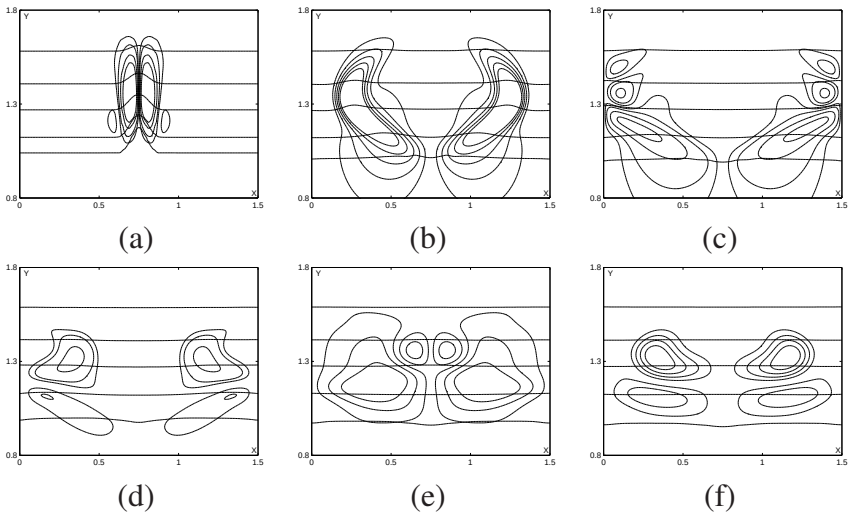

Figure 11: Level lines of the composition and of the stream function after: (a) 0.05 s, (b) 0.95 s, (c) 1.45 s, (d) 2.0 s, (e) 2.95 s, (f) 3.6 s

4.3. Numerical simulations of the complete problem

We discuss now numerical simulations of the complete problem. The variable interface width creates a force directed along the interface. This results in appearance of two vortices near the perturbation. They begin to propagate from the center of the domain to the side walls (Fig. 11 b). The concentration perturbations propagate together with the vortices. Further dynamics is similar to that for the model problem. After hitting the wall the vortices change their structure and the direction of rotation (Fig. 11 c), then they propagate to the center of the domain (Fig. 11 d), meet there, cross each other, propagate further to the walls (Fig. 11 e,f).

5. Conclusions

The question about capillary phenomena in miscible liquids was first discussed by Korteweg in the paper published in 1901. It was rather actively studied beginning from the 1990s, in particular, due to microgravity research programs. Nevertheless, the experimental confirmation of the existence of such phenomena remained arguable as well as adequate mathematical models to describe them.

An important step in the development of these studies was related to the application of the spinning drop tensiometry to IBA-water systems [34]. It allows the investigation of miscible fluids with a sharp interface between them. In this work we present two experimental evidences of capillary phenomena in miscible liquids: capillary instability and the change of the drop shape. In the first case a long cylindrical jet splits into drops, in the second case, an elliptic drop becomes spherical. Both effects are well known for immiscible liquids. In the case of miscible liquids, such behavior was not observed before.

A conventional model used to describe binary fluids consists of the Navier-Stokes equations with an additional volume force called Korteweg stress. In the case of a narrow transition zone

between two liquids, this model is equivalent to the classical interface model where two fluids are separated by an interface with jump conditions imposed at the interface [1], [23], [36]. The model based on the Korteweg stresses is more general because it allows one to consider also diffuse interfaces which are not necessarily narrow and whose width can depend on time. In this work we use this model in order to describe the capillary instability of diffuse interfaces. We also use it to show the existence of interfacial waves in miscible liquids. This theoretical result is not yet confirmed experimentally. We plan the experiments in order to do it.

Acknowledgements

Support for this research was provided by the National Science Foundation (CHE-0719099). The authors are grateful to S. Aristov and Yu. Gaponenko for their contribution to the study of interfacial waves.

References

[1] D.M. Anderson, G.B. McFadden, A.A. Wheeler. *Diffuse interface methods in fluid mechanics.* Ann. Rev. Fluid Mech., 30 (1998) 139-165.

[2] L.K. Antanovskii. *Microscale theory of surface tension.* Physical Review E, 54 (1996), No. 6, 6285-6290.

[3] D. Antrim, P. Bunton, L.L. Lewis, B.D. Zoltowski, J.A. Pojman. *Measuring the mutual diffusion coefficient for dodecyl acrylate in low molecular weight poly(dodecyl acrylate) using laser line deflection (Wiener's method) and the fluorescence of pyrene.* J. Phys. Chem. Part B, 109 (2005), 11842-11849.

[4] S. Aristov, N. Bessonov, Yu. Gaponenko, V. Volpert. *Interfacal waves in binary fluids.* In: Patterns and waves, A. Abramian, S. Vakulenko, V. Volpert, Eds., 2003, 79-97.

[5] N. Bessonov, J. Pojman, V. Volpert. *Modelling of diffuse interfaces with temperature gradients.* J. of Engineering Mathematics, 49 (2004), No. 4, 321-338.

[6] N. Bessonov, J. Pojman, V. Volpert. *Numerical simulations of transient interfacial phenomena in miscible fluids.* AIAA-2004-631, Reno. 2003.

[7] N. Bessonov, V. Volpert, J. Pojman, B.D. Zoltowski. *Numerical simulations of convection induced by Korteweg stresses in miscible polymer-monomer systems.* Microgravity Sci. Tech., XVII (2005), 8-12.

[8] J.W. Cahn, J.E. Hilliard. *Free energy of a nonuniform system. I. Interfacial free energy.* J. Chem. Phys. 28 (1958) 258-267.

[9] A. Castellanos, A. Gonzalez. *Interfacial electrohydrodynamic instability: the Kath and Hoburg model revisited.* Phys. Fluids A, 4 (1992), 1307-1309.

[10] S. Chandrasekhar. Hydrodynamic and hydromagnetic stability. Dover, New York, 1981.

[11] C.-Y. Chen, E. Meiburg. *Miscible displacements in capillary tubes: Influence of Korteweg stresses and divergence effects.* Phys. Fluids, 14 (2003) 2052-2058.

[12] B. Chu, F.J. Schoenes, M.E. Fisher. *Light scattering and pseudospinodal curves: the isobutyric-acid-water system in the critical region.* Phys. Rev. E, 185 (1969) 219-226.

[13] B. Chu, F.J. Schoenes, W.P. Kao. *Spatial and time-dependent concentration fluctuations of the isobutyric acid-water system in the neighborhood of its critical mixing point.* J. Amer. Chem. Soc., 90 (1968), 3042-3048.

[14] P. Cicuta, A. Vailati, M. Giglio. *Capillary-to-bulk crossover of nonequilibrium fluctuations in the free diffusion of a near-critical binary mixture.* Applied Optics, 40 (2001), 4140-4146.

[15] P.K. Currie, J. Van Nieuwkoop. *Buoyancy effects in the spinning-drop interfacial tensiometer.* J. Colloid Interface Sci., 87 (1982), 301-316.

[16] E.L. Cussler. Diffusion: mass transfer in fluid systems. Cambridge, 1997.

[17] H.T. Davis. *A theory of tension at a miscible displacement front. In: Numerical simulation in oil recovery.* Volumes in Mathematics and its Applications, Ed. M. Wheeler, Springer-Verlag, Berlin, 11 (1998), 105-110.

[18] P. Garik, J. Hetrick, B. Orr, D. Barkey, E. Ben-Jacob. *Interfacial cellular mixing and a conjecture on global deposit morphology.* Phys. Rev. Ltts, 66 (1991), No. 12, 1606-1609.

[19] S.G. Greer. *Coexistence curves at liquid-liquid critical points: Ising exponents and extended scaling.* Phys. Rev. A, 14 (1976), 1770-1780.

[20] M. Heinrich, B.A. Wolf. *Interfacial tension between solutions of polystyrenes: establishment of a useful master curve.* Polymer, 33 (1992), 1926-1931.

[21] M. Heinrich, B.A. Wolf. *Establishment of phase equilibria: temperature jump experiments in a spinning-drop apparatus.* Macromolecules, 26 (1993), 6106-6110.

[22] H. H. Hu, D. D. Joseph. *Evolution of a liquid drop in a spinning drop tensiometer.* J. Colloid Interface Sci. 162 (1994) 331-339.

[23] D. Jacqmin. *Contact-line dynamics of a diffuse fluid interface.* J. Fluid Mech., 402 (2000) 57-88.

[24] D.D. Joseph, Y.Y. Renardy. Lubricated transport, drops and miscible fluids, in: Fundamentals of Two-Fluid Dynamics, Springer, New-York, 1992.

[25] D.J. Korteweg. *Sur la forme que prennent les équations du mouvement des fluides si l'on tient compte des forces capillaires causées par des variations de densité considérables mais connues et sur la théorie de la capillarité dans l'hypothèse d'une variation continue de la densité.* Archives Néerlandaises des Sciences Exactes et Naturelles, 6 (1901) 1-24.

[26] I. Kostin, M. Marion, R. Texier-Picard, V. Volpert. *Modelling of miscible liquids with the Korteweg stress.* M2AN, 37 (2003) No. 5, pp. 741-754.

[27] C.D. Manning, L.E. Scriven. *On interfacial tension measurement with a spinning drop in gyrostatic equilibrium.* Rev. Sci. Instrum., 48 (1977), 1699-1705.

[28] S.E. May, J.V. Maher. *Capillary-wave relaxation for a meniscus between miscible liquids.* Phys. Rev. Ltts., 67 (1991), No, 15, 2013-2015.

[29] J.E. Mungall. *Interfacial tension in miscible two-fluid systems with linear viscoelastic rheology.* Phys. Rev. Ltts., 73 (1994), 288-291.

[30] L. Mirantsev, I. Kostin, V. Volpert. *Mean field theory of miscible liquids.* Unpublished.

[31] P. Petitjeans. *Une tension de surface pour les fluides miscibles.* C.R. Acad. Sci. Paris, Série II b 322 (1996) 673-679.

[32] P. Petitjeans. *Fluides non miscible/fluides miscibles: des similitudes intéressantes.* C.R. Acad. Sci. Paris, Série II b 325 (1997) 587-592.

[33] P. Petitjeans, T. Maxworthy. *Miscible displacements in capillary tubes. Part 1. Experiments.* J. Fluid Mech., 326 (1996), 37-56.

[34] J. Pojman, C. Whitmore, M.L. Turco Liveri, R. Lombardo, J. Marszalek, R. Parker, B. Zoltowski. *Evidence for the existence of an effective interfacial tension between miscible fluids: isobutyric acid-water and 1-butanol-water in a spinning-drop tensiometer.* Langmuir, **22** (2006) 2569-2577.

[35] J.A. Pojman, N. Bessonov, V. Volpert. *Miscible fluids in microgravity (MFMG): a zero-upmass investigation on the international space station.* Microgravity Sci. Tech., XIX (2007), No. 1, 33-41.

[36] J. Pojman, Y. Chekanov, J. Masere, V. Volpert, T. Dumont, H. Wilke. *Effective interfacial tension induced convection in miscible fluids.* Proceedings of the 39th AIAA Aerospace Science Meeting, January 2001, Reno, USA.

[37] F. Quirion, J. Pageau. *Interfacial tension between low molecular weight polymers from the static analysis of cylindrical drops and their break-up dynamics.* J. Polym. Sci.: Part B: Polym. Phys., 33 (1995), 1867-1875.

[38] I. Rousar, E.B. Nauman. *A continuum analysis of surface tension in nonequilibrium systems.* Chem. Eng. Comm. 129 (1994) 19-28.

[39] R.L. Rowley, F.H. Horne. *The behavior of the heat of transport near the critical solution temperature of isobutyric acid - water mixtures.* J. Chem. Phys., 71 (1979), 3841-3851.

[40] J.S. Rowlinson, B. Widom. Molecular theory of capillarity. Clarendon Press, Oxford, 1982.

[41] J.C. Slattery, J.D. Chen. *Alternative solution for spinning drop interfacial tensiometer.* Journal of Colloid and Interfacial Science, 64 (1978), 371-373.

[42] Y. Sugii, K. Okamoto, A. Hibara, M. Tokeshi, T Kitamori. *Effect of Korteweg stress in miscible liquid two-layer flow in a microfluidic device.* J. Visualization 2005, 8, 117-124.

[43] S. Tomotika. *On the instability of a cylindrical thread of a viscous liquid surrounded by another viscous fluid.* Proc. Roy. Soc. (London), A150 (1935), 322-337.

[44] S. Tomotika. *Breaking up of a drop of viscous liquid immersed in another viscous fluid which is extending at a uniform rate.* Proc. Roy. Soc. (London), 153 (1936), 302-318.

[45] D.H. Vlad, J.V. Maher. *Dissolving interfaces in the presence of gravity.* Physical Review E, 59 (1999), 476-478.

[46] V. Volpert, J. Pojman, R. Texier. *Convection induced by composition gradients in miscible systems.* CRAS, Serie II b, 330 (2002) 353-358.

[47] B. Vonnegut. *Rotating bubble method for the determination of surface and interfacial tensions.* Rev. Sci. Instrum., 13 (1942), 6-9.

[48] Y.B. Zeldovich. *About surface tension of a boundary between two mutually soluble liquids.* Zhur. Fiz. Khim. 23 (in Russian) (1949) 931-935.

[49] B. Zoltowski, Yu. Chekanov, J. Masere, J.A. Pojman, V. Volpert. *Evidence for the existence of an effective interfacial tension between miscible fluids. 2. Dodecyl acrylate-poly(dodecyl acrylate) in a spinning Drop tensiometer.* Langmuir, 23 (2007), 5522-5531.